In vivo autofluorescence of nasopharyngeal carcinoma and normal tissue

Jianan Y. Qu, PhD[1], Po Wing YUEN, MD[2], Zhijian Huang, PhD[1]
and William I. WEI, MD[2]

[1]Department of Electrical and Electronic Engineering, Hong Kong University of Science and Technology, Clear Water Bay, Kowloon, Hong Kong, P.R. China
[2]Division of Otorhinolaryngology, The University of Hong Kong, Queen Mary Hospital, The University of Hong Kong, 102 Pokfulam Road, Hong Kong, P.R. China

ABSTRACT

An optical imaging and spectroscopy system has been developed for the study of *in vivo* fluorescence of nasopharngeal tissue through an endoscope. The system records the fluorescence signal in the imaging plane of the endoscopic system. This allows analyze the characteristics of the light induced fluorescence (LIF) spectra recorded by each pixel of the two dimensional detector which may be used for fluorescence endoscopic imaging. If the endoscope for fluorescence endoscopy is the same as one employed for the *in vivo* fluorescence study, the algorithms developed to distinguish the diseased tissue from normal tissue based on the *in vivo* fluorescence study should be highly reliable for fluorescence imaging of lesions. In this work, fluorescence spectra were collected from 27 full term patients. Different algorithms were tested for separation of cancerous lesions from normal tissue. High sensitivity and specificity were achieved.

Keywords: Fluorescence, spectroscopy, imaging, cancer

1. INTRODUCTION

Nasopharyngeal carcinoma (NPC) occurs with highest incidence and frequencies in Asian countries. Genetic factors, infection with the Epstein-Barr virus (EBV), and environmental factors are all implicated as being important for the development of NPC[1-4]. Screening of nasopharyngeal carcinoma is now carried out by checking individuals suspected of having NPC for elevated levels of serum IgA antibodies directed against EBV viral capsid antigen (VCA) and Early Antigen(EA) with subsequent nasoendoscopic biopsy of the nasopharynx. However, many malignant tumors and early lesions such as carcinoma *in situ* are small and have the flat surface. It is difficult to localize the small and flat lesions with an ordinary endoscopy. Random biopsies are usually conducted to screen for subclinical tumors. According to the statistic results, only 5.4% of patients with elevated serum EBV antibody titer had asymptomatic NPC in random biopsy of the nasopharynx[3]. The low incidence of pathological evidence of nasopharyngeal carcinoma suggests that majority of the screening program will suffer the unnecessary trauma caused by the random biopsy. Furthermore, patients with raised serum EBV antibody titer or with tumor removed need to have follow-up endoscopy and biopsy to rule out possible nasopharyngeal carcinoma, residual tumor or tumor recurrence. As a result, a remote imaging technique is desirable for early detecting malignant tumor and guiding the routine biopsy procedure.

Laser-induced fluorescence (LIF) of tissues depends on their biochemical and histomorphologic characteristics. LIF technology has already successfully demonstrated the capability to distinguish normal tissue from precancerous and early cancerous lesions at different human organs and body sites. Optical fiber probes were most commonly used for *in vivo* LIF spectroscopic study of tissue. However, the fluorescence imaging technique such as fluorescence endoscopy is more desirable and convenient for clinical diagnosis. The optics of endoscope is very different from fiber probe in terms of optical illumination and collection geometry. The endoscope collects information from much larger area than optical fiber probe used of point measurement. To separate the normal tissue from lesions, the algorithm for fluorescence image processing should be created based on the correlation between fluorescence spectra and pathologic results. The fluorescence spectra should be recorded from the location where the biopsy is taken for pathologic diagnosis. Also, the spectra must be collected by a system with the same geometry as endoscope employed. In this work, we built a multiple channel spectrometer for the study of characteristics of *in vivo* fluorescence signal recorded by an imaging system. Specifically, the spectrometry analyzed the LIF signal of tissue in the image plane of a conventional endoscopic system

during endoscopy. This allowed us to investigate the fluorescence signal received by each pixel of a two dimensional sensor proposed for recording the LIF image of the fluorescence endoscopy. First, we created a simple algorithm to detect nasopharyngeal carcinoma by using the ratio of fluorescence signals at two wavelength bands. Furthermore, we tested the algorithm involved with the fluorescence signals at three wavelength bands to compensate for the effect of blood absorption on the fluorescence signal. The performance of the algorithm should be more stable with reducing the distortion of tissue fluorescence signal by the variation of blood content. Finally, we discuss the possibility to further improve the sensitivity and specificity of the LIF imaging technique. Instead of using a general algorithm built on the spectral data collected from a group of subjects, we propose to make use of the difference of fluorescence signals between diseased and normal tissue within an individual to create a more robust algorithm for the detection of diseased tissue.

2. MATERIALS AND METHODS

The schematic diagram of the imaging and spectroscopy system for study of *in vivo* fluorescence signal is shown in Figure 1. The system was designed to be able to adapted to any endoscope. A 100 W mercury arc lamp filtered by a band pass filter in the wavelength range from 390 nm – 450 nm was used as excitation source. The excitation power at the endoscope tip is about 50 mW. The fluorescence and reflection of excitation from the tissue surface were imaged by a commercial endoscope. A dichroic mirror with cut-on wavelength at 470 nm divided the optical signal from the endoscope into the reflection and fluorescence channels. The image recorded by a CCD video camera in reflection channel was displayed on a monitor for the real time endoscopy. A long pass filter with cut-off wavelength at 470 nm was used to eliminate residual excitation light in the fluorescence channel. The fluorescence signal was collected by an optical fiber bundle with seven optical fibers of 200 μm in diameter and NA 0.16. The fibers were evenly distributed in fluorescence image plane of the endoscope. When the separation of the endoscope distal tip and the imaged tissue surface was 15 mm, each single fiber sampled the signal from the area about 1mm in diameter on tissue surface. The sampling area is much smaller than the total illuminated area. The fluorescence signals received by the fibers were conducted to the entrance slit of an imaging spectrograph. The tips of optical fibers were placed in the entrance plane and lined up vertically. The fluorescence conducted by the fibers were then dispersed and imaged onto an intensified CCD (ICCD) camera. The images of CCD and ICCD were grabbed simultaneously by a frame grabber at rate of 25 frames per second. The spectra of a white light lamp shown in Figure 2a were formed by binning the seven spectral strips in the image vertically. The wavelength of the spectral measurement was calibrated by using a standard spectral lamp. The response of ICCD with fixed gain was in its linear region. A typical image grabbed from real time video with aiming marks is shown in Figure 2b.

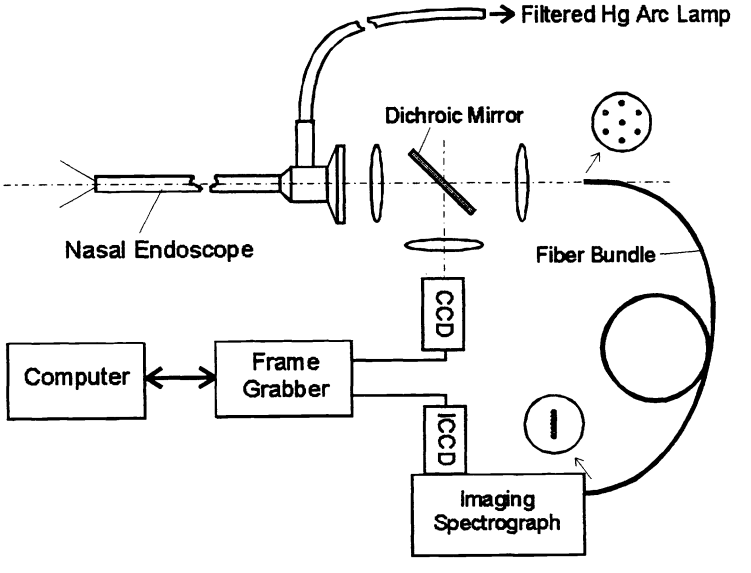

Figure 1. Arrangements for *in vivo* measuring tissue autofluorescence in the image plane of a nasal endoscopic imaging system.

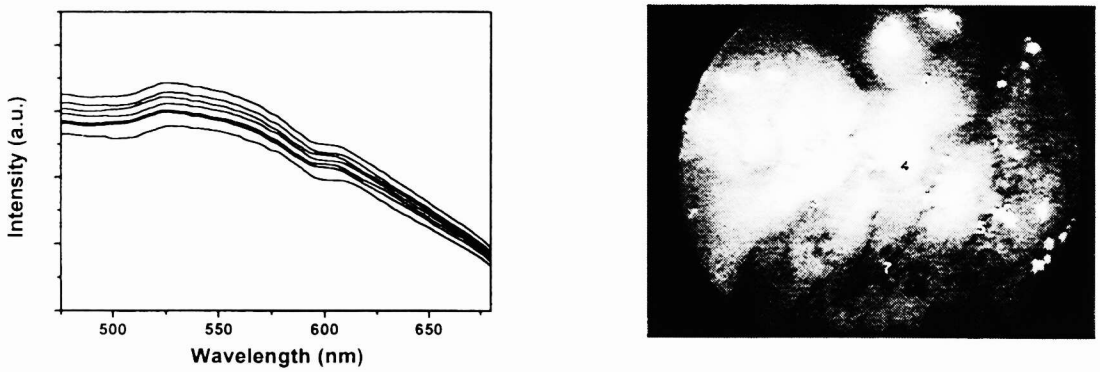

Figure 2. (a) Spectra formed by binning the spectral strips vertically. (b) Real time image recorded from the endoscope overlaid with aiming number marks of seven optical fibers. Each mark indicates the area aimed by a correspondent single fiber. Fluorescence signals are collected from seven sampling areas simultaneously. The highlighted number points the area of interest on the tissue surface where both fluorescence measurement and biopsy will be taken.

The *in vivo* fluorescence measurements have been conducted in the Department of Otorhinolaryngology and Department of Clinical Oncology at Queen Mary Hospital, The University of Hong Kong. A total of 27 subjects were enrolled in this study which lasted about six months. The fluorescence spectra were measured at the sites where biopsy specimens were taken. Histologic examinations on biopsies were then performed by the pathologists. This study was approved by the Ethical Committee of Queen Mary Hospital, the University of Hong Kong.

3. RESULTS AND CONCLUSIONS

We collected *in vivo* fluorescence on 110 biopsy sites from 27 subjects before the biopsy procedures were performed. In which, 58 were found to be normal, 52 exhibited carcinoma. Figure 3 illustrates typical fluorescence spectra acquired from nasopharyngeal sites. All fluorescence intensities are not calibrated due to variation of measurement geometry site by site. As can be seen, the spectral lineshapes vary not only individual by individual but within individual also. The peak emission wavelength of nasopahryngeal carcinoma and normal tissue occurs within ±10 nm of 510 nm. The large variation of fluorescence intensity in the region of 530 – 590 nm and peak emission wavelength indicates that the blood content in tissue plays important role in the distortion of fluorescence signal recorded on the tissue surface[11,12,19,20]. During the fluorescence measurement procedure, the distance between the distal tip of endoscope and tissue surface was kept in the range from 10 to 15 mm. Although the distance was not calibrated, we observed that the fluorescence intensity from the nasopahryngeal carcinoma was generally lower than the normal tissue.

A simple algorithm based on the ratio of fluorescence signals at two wavelength bands was created to differentiate the nasopharyngeal carcinoma from the surrounding normal tissue. As discussed previously, the algorithm will be valid for the fluorescence endoscopic imaging system because the tissue fluorescence were analyzed in the image plane of the endoscope. A set of wavelength bands in the range from 470 – 700 that best separated the carcinoma and normal tissue was found by exhaustive search. The minimal bandwidth was set to 30 nm in the search. A very narrow bandwidth becomes not practical because the signal to noise ratio SNR is inversely proportional to the bandwidth and the performance of a fluorescence imaging system is strongly dependent on the SNR. The ratio of fluorescence signal in the short wavelength band vs. long wavelength band was calculated. An unpaired student's *t*-test was used to compare the ratio scores of the normal and carcinoma tissues. The separation of normal tissue from carcinoma was evaluated by the student's *t*-test result. The optimal wavelength bands for the ratio algorithm was found at 500±25 nm and 640±40 nm as shown in Figure 3. The ratio scores of the signals in the band of 500±25 nm vs. 640±40 nm from all measured fluorescence spectra are shown in Figure 4a. The distributions of the ratio scores for normal and carcinoma are displayed separately because of the slight

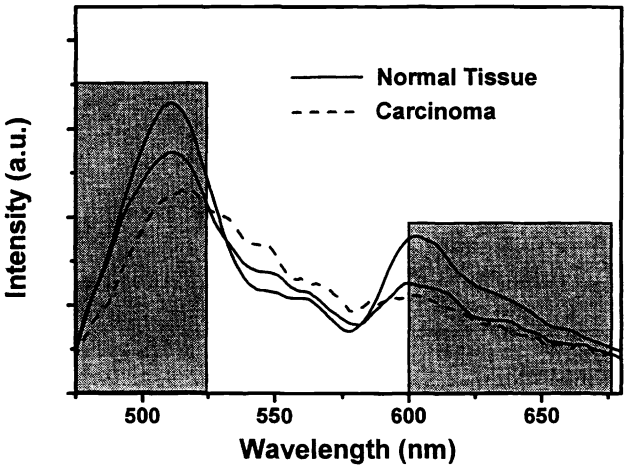

Figure 3. Typical *in vivo* autofluorescence emission spectra

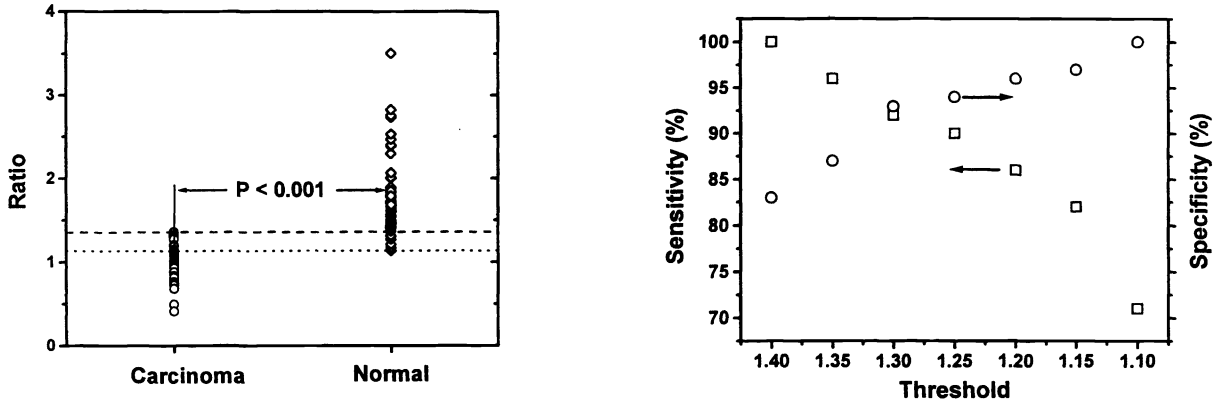

(a) (b)

Figure 4. (a) Scatter plot for the scores of two wavelengths ratio algorithm. The circles and diamonds represent the scores of nasopharyngeal carcinoma and normal tissue, respectively. (b) Dependence of sensitivity and specificity of two wavelengths algorithm on the diagnostic threshold. The squares and circles represent the sensitivity and specificity, respectively.

overlapping between two groups. The mean ratio scores were 1.78±0.48 for normal nasopharyngeal tissue and 0.99±0.20 for the carcinoma. The *p*-value of student's *t*-test on the ratios for normal tissue and carcinoma was found to be smaller than 0.001. This indicates the significantly statistical difference (P<0.001) between two groups of scores. To further evaluate the performance of two wavelengths algorithm, we calculated the sensitivity and specificity of the algorithm as a function of decision thresholds. The sensitivity and specificity were defined as

$$Sensitivity = \frac{True\ \ Positives}{True\ \ Positives + False\ \ Negatives}$$

$$Specificity = \frac{True\ \ Negatives}{True\ \ Negatives + False\ \ Positives}$$

The dash and dot lines in Figure 4a represent the diagnostic thresholds for sensitivity of 100% and specificity of 100%, respectively. The dependence of sensitivity and specificity on diagnostic threshold are shown in Figure 4b. As can be seen, when the threshold is set to 1.30, the two wavelengths algorithm can achieve both sensitivity and specificity about 92%.

As discussed in the beginning of the section, the variation of blood content plays an important role in distortion of fluorescence spectra emitted from tissue surface. The result of an exhaustive search of the optimal set of wavelength bands for the ratio algorithm has reflected the effect of blood content on the fluorescence measurement. The optimal set of wavelength bands at 500±25 nm and 640±40 nm excludes the wavelength region of 530nm to 590 nm where the blood appears very strong absorption[19,20]. This indicates that the exhaustive search is a process to minimize the blood effect on the performance of the ratio algorithm. However, the absorption coefficient of blood in the wavelength band of 500±25 nm is still much greater than 640±40 nm[19,20]. To further reduce the effect of blood absorption and improve the accuracy of the diagnosis, we investigated an algorithm which compensated the variation of fluorescence signal in wavelength band of 500±25 nm caused by blood absorption to some extent.

The algorithm was created by forming the dimensionless function

$$R = \frac{I(500 \pm 25)}{I(640 \pm 40)}\left(\frac{I(500 \pm 25)}{I(560 \pm 35)}\right)^{k}$$

in which fluorescence signals in three wavelength bands: 500±25 nm, 560±35 nm and 640±40 nm were employed. The first term of R-function is the two wavelengths ratio. The second term includes the information of blood absorption and is used to compensate the effect of blood variation on the first term. A constant k was used to scale the blood effect on the score of the algorithm. It has been found in an exhaustive search that the best separation was achieved by setting the value of k about 0.51. Again, the result of an unpaired student's t-test was used as the criterion to determine the best separation and optimal value of constant k. The scores of R-function for normal and carcinoma tissues are shown in Figure 5a. The mean scores of R-function for normal and carcinoma tissues are 1.95±0.50 and 1.00±0.21, respectively. The small p-value (<0.001) demonstrates that the significantly statistical difference between two groups of scores. It has been noticed that the variances of R-function scores for normal and carcinoma tissues are at the same levels as the two wavelengths algorithm. However, the difference of mean score between the normal tissue and carcinoma is 0.95, compared to 0.79 of two wavelengths algorithm. This indicates that three wavelengths algorithm can separate the normal tissue and carcinoma better than two wavelengths algorithm. The dependence of sensitivity and specificity on the diagnostic threshold for three wavelengths algorithm is displayed in Figure 5b. The sensitivity of 98% and specificity of 95% can be achieved when the threshold is set to 1.35.

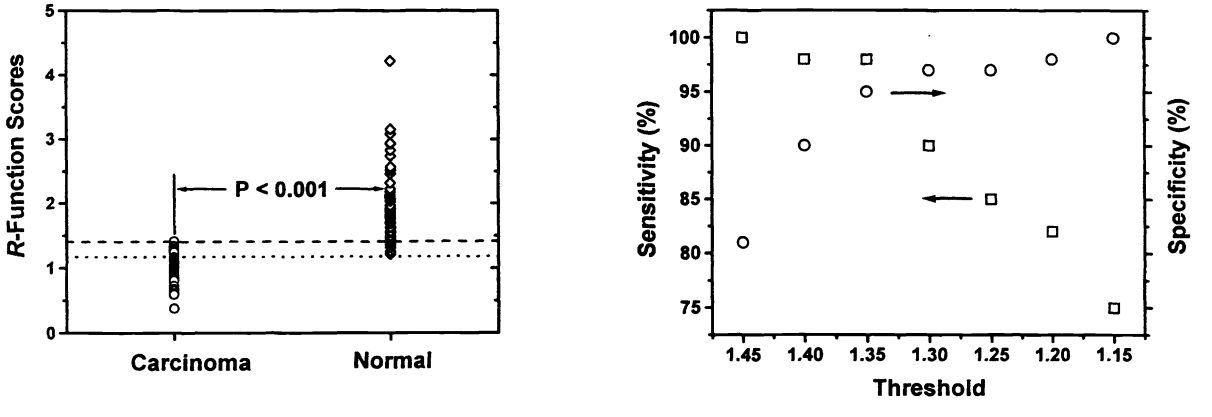

(a) (b)

Figure 5. (a) Scatter plot for the scores of three wavelengths ratio algorithm. The circles and diamonds represent the scores of nasopharyngeal carcinoma and normal tissue, respectively. (b) Dependence of sensitivity and specificity of three wavelengths algorithm on the diagnostic threshold. The squares and circles represent the sensitivity and specificity, respectively.

In conclusion, we built a multiple channel spectrometer to analyze the light induced fluorescence spectra of nasopahryngeal carcinoma and normal tissue in the image plane of a standard nasal endoscope. The results of the study reported here demonstrate that a conventional endoscopic system with the feature of fluorescence spectral imaging can localize the naspharyngeal carcinoma with high sensitivity and specificity. There is not a technical obstacle and cost problem to build a two wavelengths and three wavelengths imaging system for real time endoscopy[15-18]. The fluorescence endoscopy will offer unique information for the early detection of maligant nasopahryngeal tumors noninvasively. The method to investigate the tissue autofluorescence in our study can be generally used to create reliable algorithm for various fluorescence endoscopic imaging systems to detect diseased tissue on other organ sites. It should be pointed out that no subject with a subclinical cancerous lesion was found and examined in this six months pilot study. The pathological analysis showed that all biopsied sites, where the *in vivo* fluorescence spectra were measured, exhibited either normal or invasive carcinoma, although some carcinoma lesions are flat and unobservable. Furthermore, the exact biochemical and morphological basis for the difference in fluorescence spectral characteristics between normal and carcinoma tissue are currently unknown. In the future study, we will focus on investigating the autofluorescence of early lesion and develop the understanding of the basis of nasopharyngeal autofluorescence.

4. REFERENCES:

1. Ho JHC. Genetic and environmental factors in nasopharyngeal carcinoma. In: W. Nakahara et al, eds. Recent Advances in Human Tumor Virology and immunology. Tokyo: University of Tokyo Press. 1971:275-95.
2. Ho JHC, Ng MH, Kwan HC, Chau JCW. Epstein-Barr virus-specific IgA and IgG serum antibodies in nasopharynageal carcinoma. Br J Cancer 1976; 34: 655-9.
3. Wei WI, Sham JS, Zong YS, Choy D, Ng MH. The efficacy of fiberoptic examination and biopsy in the detection of early nasopharyngeal carcinoma. Cancer 1991; 67: 3127-3130.
4. Sham JS, Wei WI, Kwan WH, Chan CW, Kwong WK, Choy D. nasopharyngeal carcinoma - pattern of tumor regression after radiotherapy. Cancer 1990; 65:21.
5. Wagnieres GA, Star WM, Wilson BC. In vivo fluorescence spectroscopy and imaging for oncological applications. Photochemistry & Photobiology. 1998; 68:603-32.
6. Cothren RM, Richards-Kortum R, Sivak MV Jr., Fitzmaurice M, Rava RP, Boyce GA, Doxtader M, Blackman R, Ivanc TB, Hayes GB, Doxtader M, Blackman R, Ivanc T, Feld MS, Petras RE. Gastrointestinal tissue diagnosis by laser-induced fluorescence spectroscopy at endoscopy. Gastrointestinal Endoscopy. 1990; 36:105-11.
7. Hung J, Lam S, LeRiche JC, Palcic B. Autofluorescence of normal and malignant bronchial tissue. Lasers in Surgery & Medicine. 1991; 11: 99-105.
8. Ramanujam N, Mitchell MF, Mahadevan A, Thomsen S, Silva E, Richards-Kortum R. Fluorescence spectroscopy: a diagnostic tool for cervical intraepithelial neoplasia (CIN). Gynecologic Oncology. 1994; 52: 31-38
9. Qu J, MacAulay C, Lam S, Palcic B. Laser-induced fluorescence spectroscopy at endoscopy: tissue optics, Monte Carlo modeling, and in vivo measurements. Opt. Eng. 1995; 34: 3334-3343.
10. Zeng HS, Weiss A, Cline R, MacAulay CE. Real time endoscopic fluorescence imaging for early cancer detection in the gastrointestinal tract. Bioimaging. 1998; 6: 151-165.
11. Wu J, Feld MS, Rava RP. Analytical model for extracting intrinsic fluorescence in turbid media. Appl. Opt. 1993; 32:3585-3595
12. Gardner CM, Jacques SL, Welch AJ. Fluorescence spectroscopy of tissue: recovery of intrinsic fluorescence from measured fluorescence. Appl. Opt. 1996; 35: 1780-1792
13. Ramanujam N, Mitchell MF, Mahadevan A, Thomsen S, Malpica A, Wright T, Atkinson N, Richards-Kortum R. Development of a multivariate statistical algorithm to analyze human cervical tissue fluorescence spectra acquired in vivo. Lasers in Surgery & Medicine. 1996; 19:46-62
14. Tumer K, Ramanujam N, Ghosh J, Richards-Kortum R. Ensembles of radial basis function networks for spectroscopic detection of cervical precancer. IEEE Transactions on Biomedical Engineering. 1998; 45:953-61.
15. Andersson-Engels S, Johansson J, Svanberg K, Svanberg S. Fluorescence imaging and point measurements of tissue: applications to the demarcation of malignant tumors and atherosclerotic lesions from normal tissue. Photochemistry & Photobiology. 1991; 53:807-14.
16. Palcic B, Lam S, Hung J, MacAulay C. Detection and localization of early lung cancer by imaging techniques. Chest. 1991; 99:742-3.

17. Andersson-Engels S, Johansson J, Svanberg S. Medical diagnostic system based on simultaneous multispectral fluorescence imaging. Applied Optics, 1994; 33: 8022-8029.
18. Wagnieres GA, Studzinski AP, van den Bergh HE. An endoscopic fluorescence imaging system for simultaneous visual examination and photodetection of cancers. Rev. Scient. Inst. 1997: 68: 203-212.
19. van Kampen EJ, Zilstra WG. Determination of hemoglobin and its derivatives. In: H. Sobotka and C. P. Stewart, eds. Advances in Clinical Chemistry. New York: Academic. 1965: 8:158-187.
20. van Assendelft OW. Spectrophotometry of haemoglobin derivatives. Netherlands: Royal Vangorcum Ltd. 1970: 55-70.
21. Gonzalez RC, Woods RE. Digital imaging processing. New York: Addison-Wesley Pub. Co. Inc. 1993: 413-477.